

IN-34
163046
p.28

NASA Technical Memorandum 106129

An Extended Lagrangian Method

Meng-Sing Liou
Lewis Research Center
Cleveland, Ohio

May 1992

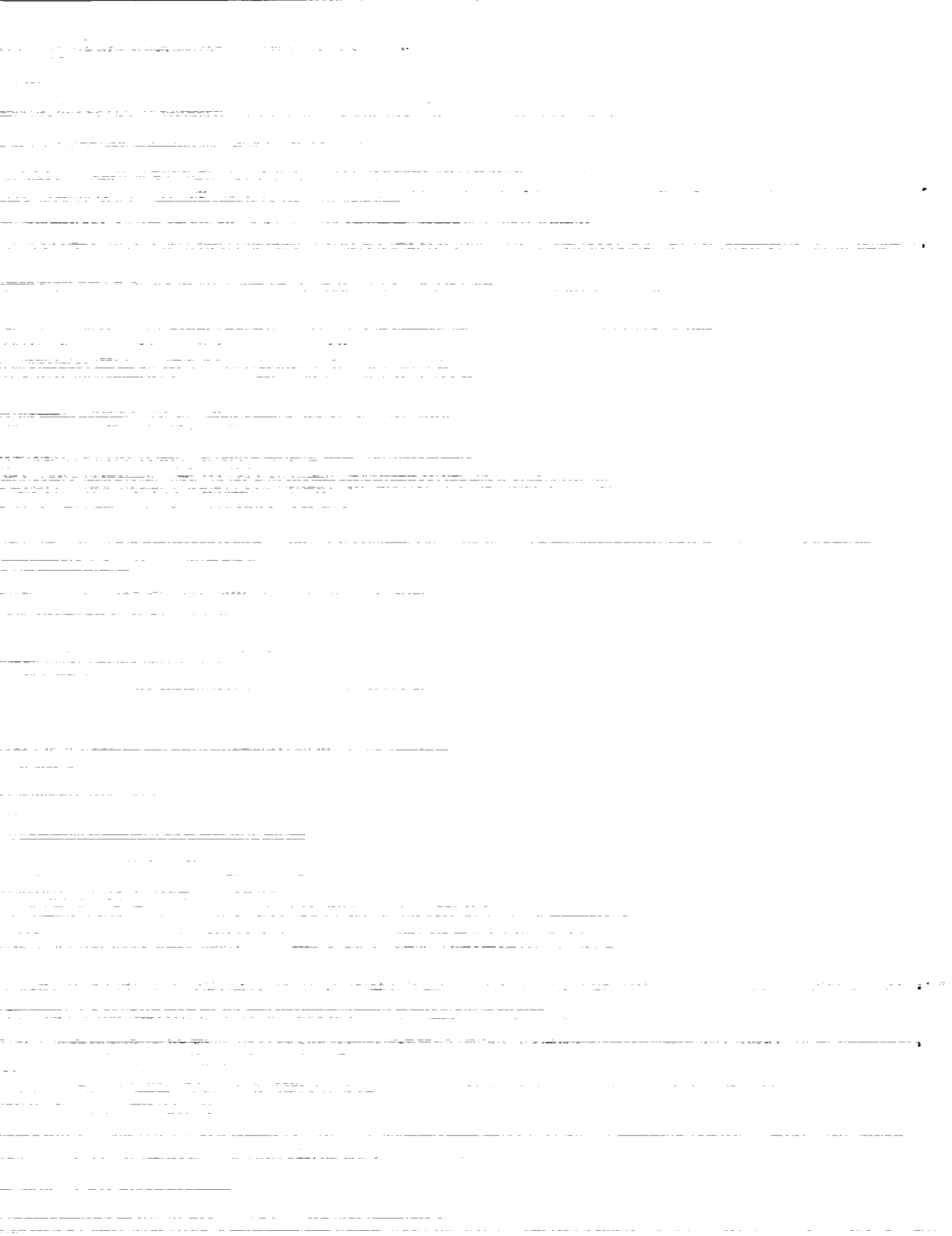
(NASA-TM-106129) AN EXTENDED
LAGRANGIAN METHOD (NASA) 28 p

N93-26203

Unclas

G3/34 0163046





AN EXTENDED LAGRANGIAN METHOD

Meng-Sing Liou†

National Aeronautics and Space Administration

Lewis Research Center

Cleveland, Ohio 44135

ABSTRACT

A unique formulation of describing fluid motion is presented. The method, referred to as "extended Lagrangian method," is interesting from both theoretical and numerical points of view. The formulation offers accuracy in numerical solution by avoiding numerical diffusion resulting from mixing of fluxes in the Eulerian description. Meanwhile, it also avoids the inaccuracy incurred due to geometry and variable interpolations used by the previous Lagrangian methods [1,2]. Unlike the Lagrangian method proposed in [3,4] which is valid only for supersonic flows, the present method is general and capable of treating subsonic flows as well as supersonic flows. The method proposed in this paper is robust and stable. It automatically adapts to flow features without resorting to clustering, thereby maintaining rather uniform grid spacing throughout and large time step. Moreover, the method is shown to resolve multi-dimensional discontinuities with a high level of accuracy, similar to that found in one-dimensional problems.

1. INTRODUCTION

It is well known that fluid motion can be specified by either the Eulerian or Lagrangian description. Most CFD developments over the last three decades have been based on the Eulerian description and considerable progress has been made. In particular, the upwind methods, inspired and guided by the work of Gudonov[5], have met with a great deal of success in solving fluid flows, especially where discontinuities exist. However, this shock capturing property has proven to be accurate only when the discontinuity is aligned with one of the grid lines since most upwind methods are strictly formulated in a one-dimensional framework and only formally extended to multi-dimensions. Consequently, the attractive property of crisp resolution of these discontinuities is lost. Even though research on genuine multi-dimensional approaches has recently been undertaken by several leading researchers, they are nevertheless still based on the Eulerian description.

Recently, Loh and Hui[3] have convincingly demonstrated that a Lagrangian formulation can capture a contact discontinuity crisply, which is difficult to achieve by Eulerian formulation without resorting to some special treatment such as sub-cell resolution. Further developments have been carried out by Loh and Liou to solve real gas problems[6]

† Senior Scientist, Internal Fluid Mechanics Division.

and three-dimensional supersonic problems[4]. The 3D extension is not so trivial and in fact it involves somewhat tricky definition of cell movement and approximate solution of the multi-dimensional Riemann problem. Several interesting 3D problems that have not been attempted previously were calculated and again as in the 2D case, high accuracy was achieved in resolving very complex shock-shock interactions. This method employs the point of view that it *strictly* follows the fluid particles released at some initial time line. The streamlines become a “time-like” coordinate and are used also for identifying particles. Therefore the method is naturally suitable for supersonic steady flow. No grid generation is needed a priori since the grid is a part of the solution, viz new grid lines are obtained as the solution marches in the “time-like” direction. Unfortunately, restriction to supersonic flows only limits the use of the method. To include the subsonic regime requires substantial conceptual changes.

Numerically solving *subsonic flows* using the strict Lagrangian concept becomes an excessive obstacle. Numerous researchers at Los Alamos, making substantial contributions to this subject, have proposed the so-called Arbitrary Lagrangian-Eulerian(ALE) method, for example [1,2] and others. The method consists of three phases of numerical procedures, using time-splitting approximations, and can become rather complicated and tedious. Tracking the Lagrangian cells requires interpolations of data and coordinates. Additional constraints must be imposed to prevent grid lines from crossing each other during the rezoning. Loss of accuracy is then inflicted through the continuous geometry and flow interpolations in response to the fluid particle motion. Indeed, such a Lagrangian procedure finds some analogy in the shock fitting procedure, although the former is more complicated.

Physically fluid particles seem to adjust to motion and to surrounding (geometric or physical) constraints quickly and graciously, in particular sensing the upstream-propagating influences. Thus, a key to the success of a numerical Lagrangian procedure lies in how to properly and instantaneously feed these upstream-propagating waves to the particles, while tracking them. It is indeed a very challenging research topic that motivates us to begin this exploratory investigation. This paper presents the salient features of the method, referred to as “extended Lagrangian method”. For flows at all speed regimes including purely subsonic and mixed flows, we demonstrate the advantages of the method over the Eulerian description, with focuses on important features commonly seen in compressible flows, such as shocks, expansion waves, slip surfaces, and interactions among them. We list the distinct features resulting from the extended Lagrangian method.

1. The solution adapts to the flow variations (smooth or sudden), notably shocks and contacts, and as such it can be regarded as an automatic procedure for solution adaptation.
2. Unlike the conventional adaptation techniques, there is no need for clustering grid points near the discontinuities. Very uniform grid can be maintained and in fact can also achieve orthogonality easily by construction. Thus discretization accuracy does not deteriorate. Since streamlines do not cross, grid singularity or negative volume certainly will not occur.

3. As will be seen later, the shock capturing quality in 2D is comparable to that found in the 1D problem. This suggests that the present approach can be viewed as an alternative to the current genuine multi-dimensional approach.
4. The contact discontinuity can be resolved crisply, since it is a streamline and as such no numerical diffusion is introduced due to fluid crossing the cell face.

The rest of the paper is organized as follows. In Section 2 we compare differences of Eulerian and Lagrangian descriptions of fluid motion, with an emphasis on the numerical aspects. Some current Lagrangian approaches are commented on in Section 3. Section 4 outlines the key elements in formulating the present extended Lagrangian method for solving *subsonic* flows by retaining the advantageous features of the Lagrangian approach. A detailed formulation is then given in Section 5, including the discretization method and boundary conditions. Section 6 describes the grid motion of the present "extended Lagrangian" method. Finally, in Section 7 we demonstrate the advantages of the proposed method by displaying solutions of flows at all speed regimes, containing various interesting features.

2. EULERIAN VS LAGRANGIAN DESCRIPTION

By definition, the Eulerian description observes at *fixed locations* the flow properties as fluid particles pass by. This has a close relation to the conventional computation approach in that each fixed grid point can be thought of as an observing station—corresponding to probes in measurement. With this approach, the meshes are generated mainly based on the geometry constraint, with little regard given to the motion of fluid. Naturally, the grid lines will seldom coincide with fluid path lines. Even when grid lines are clustered near high-gradient regions using conventional adaptation techniques, they are not aligned with the particle path. A good example is the shock wave along which grid lines are densely distributed, and with which streamlines make a nonzero angle, since the fluid will always pass through, not along, the shock wave. The angle is usually oblique in multidimensional flows. Consequently, the Eulerian approach has several severe numerical effects on the solution accuracy:

1. Fluid particles are free to cross the grid line, thereby bringing (convecting) with them numerical mixing and diffusion across the cell interface.
2. This numerical diffusion is only associated with the error resulting from approximating the *convective terms*.
3. A contact/slip or shear layer is smeared ever increasingly with time and distance, unless some detection and special treatment techniques are employed. See [7] for example.

In spite of numerical diffusion resulting from approximation of convective terms, the Eulerian description does offer convenience and simplicity both conceptually and geometrically. The grid can be constructed regularly, simply based on geometry constraints and

independent of flow features. To enhance accuracy, grid adaptation is often applied to regions of high gradients. However, the concept of adapting to high gradients inevitably results in a skewed and distorted grid. This feature will become more troublesome as two or more high-gradient areas intersect.

It is quite safe to say that during the last three decades CFD algorithm researchers have primarily concentrated on developing better (more accurate/robust/efficient) ways to deal with the *convective terms*, which exist only in the Eulerian formulation. Consequently, much success has been achieved, perhaps to the point of near perfection and little return could be gained. Unfortunately, inaccuracy due to numerical diffusion(mixing) in forming the interface numerical fluxes still exists and becomes more exaggerated in multi-dimensional problems. On the other hand, since the convective terms do not explicitly appear in the Lagrangian formulation, the numerical mixing automatically disappears in the flux evaluation, rendering the Lagrangian approach more attractive. However, some other technical barriers have surfaced and discouraged researchers from further pursuing development of methods for this approach. In what follows, we shall detail the concept of the Lagrangian approach from the viewpoint of numerical solution. The differences between the two descriptions will then become obvious.

The Lagrangian description, by definition, states the motion and properties of *given* fluid particles as they travel to different locations. In particular, since the particle path in steady flow coincides with the streamline, no fluid particles will cross the streamline. In other words, while staying in contact, neighboring streams will not mix via convection, except in the molecular level where the physical molecular diffusion takes place. Therefore, the following numerical consequences can be realized:

1. No numerical diffusion is introduced across the cell interface since the computational cells follow the streamline.
2. Fluid particles change motion (direction/speed) only as warranted, e.g., as shock or expansion waves are encountered. In other words, streamlines will bend, converge, or diverge only as situations demand.
3. This description gives a realistic depiction of flow behavior; cells of same j -index form a streamline that is identifiable with flow visualization.

The notion of using a Lagrangian approach to describe flow is not new. In fact, the very essence of following *fixed* particles also presents mathematical complexity to the approach, thereby limiting its scope of success. With the help of the new Lagrangian formulations, numerical solution can be as easily obtained as for the Eulerian approach, only with the additional distinct advantages as stated above. In the following, we shall first review some current numerical procedures based on the Lagrangian approach, commenting about their strengths and weaknesses. Then we will focus on the applicability to the more difficult problem, namely the subsonic regime.

3. REVIEW OF CURRENT LAGRANGIAN APPROACHES

The Arbitrary Lagrangian-Eulerian Technique (ALE) perhaps is the most well-known Lagrangian formulation in use at present time. The technique, initially conceived and developed at Los Alamos during the 70s and further implemented in the production codes such as CAVEAT and KIVA[8,9], etc., consists of three phases of numerical procedures using the time splitting concept. For a complete description of the procedure, the reader is referred to Refs.[1,2,8,9]. Continuous rezoning is carried out in order to follow the particle motion. As a result, spurious error produced by this procedure can lead to grid irregularity and tangling. Thus loss of accuracy, manifested as numerical diffusion, is inflicted through geometry and flow variable interpolations.

Recently a new Lagrangian Formulation was proposed by Hui and Van Roessel [10]. The inviscid conservation laws are transformed by using stream functions and Lagrangian time as independent variables. The stream functions serve to identify particles, while Lagrangian time represents time-like coordinate. Under this formulation, geometry conservation is enforced and each cell is literally a fluid particle. Since there is no need for remapping, the associated loss of accuracy seen in the ALE method does not appear, allowing extremely sharp resolution of contact discontinuities. Successful demonstrations have been made by Loh and Hui [3] in 2D and Loh and Liou [4] in 3D problems. Multi-dimensional discontinuities are resolved with the same level of accuracy as their one-dimensional counterparts, indicating that the Lagrangian formulation inherently includes multi-dimensional flow characteristics. However, a severe limitation restricts the validity of the formulation [3,4] to only *supersonic flows* because the formulation is based on the use of the time-like coordinate. Thus, extension to *subsonic flows* based on the same framework appears impossible. In what follows we will first give the basic ideas for extension in the next section and then describe detailed steps in Section 5.

4. EXTENSION TO SUBSONIC FLOWS

A key element in the *subsonic flow* is the existence of the upstream-propagating wave. Thus, the existence of a body located downstream is transmitted to the oncoming fluid particles via this wave so that the particles can change motion accordingly. This immediately implies that we must abandon the time-like formulation since it is only suited for pure initial value problems, such as supersonic flow where no influence comes from downstream. Next, we must also abandon the idea of following a fixed particle, at least for the steady flows. Alternatively, we consider the steady streamlines as a set of lines that are occupied by particles released at the same location, different times and yet treated indistinguishably. The upstream-propagating influence is felt through the downstream particles on the same streamline in order to satisfy the governing conservation equations and boundary conditions in question. By describing fluid motion along streamlines, we allow fluids to *maintain*

their identity without tracking each specified particle. This definition is of course broader than and is a sufficient condition to the Lagrangian description, which follows motion of fluids of specific identity. Consequently, the present method is termed *extended Lagrangian* method. The net result is that we retain the essential beauty of the Lagrangian description that introduces no or minimal numerical diffusion across streamlines.

5. APPROACH

To facilitate the description, let us first define the notation for the relevant variables in the 3D Euler equations. The physical variables in a phase space of dimension 5 are denoted by a boldface uppercase letter or column vector whose elements are denoted by lowercase letters.

$$\mathbf{U} = \begin{pmatrix} \rho \\ \rho u \\ \rho v \\ \rho w \\ \rho e_t \end{pmatrix}, \quad \mathbf{U}_c = \begin{pmatrix} \rho \\ \rho u \\ \rho v \\ \rho w \\ \rho h_t \end{pmatrix}, \quad (1)$$

where $e_t = e + 0.5(u^2 + v^2 + w^2)$ and $h_t = e_t + p/\rho$. The geometrical vectors in physical (Cartesian) space of dimension 3 are denoted by an overhead arrow " $\vec{}$ ". The fluid velocity is

$$\vec{V} = u\vec{i} + v\vec{j} + w\vec{k}, \quad (2a)$$

and the normal vector of the boundary surface of a control volume

$$\vec{S} = s_x\vec{i} + s_y\vec{j} + s_z\vec{k}. \quad (2b)$$

The inviscid fluxes in 3D physical space are compactly written as

$$\vec{F} = \begin{pmatrix} \rho \\ \rho u \\ \rho v \\ \rho w \\ \rho h_t \end{pmatrix} \vec{V} + \begin{pmatrix} 0 \\ p\vec{i} \\ p\vec{j} \\ p\vec{k} \\ 0 \end{pmatrix} = \mathbf{U}_c \vec{V} + \vec{P}, \quad \text{where } \vec{P} = \begin{pmatrix} 0 \\ p\vec{i} \\ p\vec{j} \\ p\vec{k} \\ 0 \end{pmatrix}. \quad (3)$$

The first term in \vec{F} is the flux of \mathbf{U}_c convected by the fluid velocity \vec{V} and the second term simply the pressure flux.

For the following discussion, it is useful to review some basic concepts used to describe fluids. It is understood that the fluid has been considered to be a continuum. A convenient concept within continuum mechanics for describing a fluid motion is that of *control volume*. In Fig. 1, let $\Omega^*(t)$ be a moving volume with bounding surface $\partial\Omega^*(t)$; the local boundary velocity is \vec{V}_b . The volume is arbitrary and in general need not be identified with either

physical boundary or specific motion of the fluid in Ω^* . Such a volume is called control volume. A special type of control volume is called material volume, denoted by $\Omega(t)$, consisting of a collection of matter of fixed identity enclosed by a material surface, denoted by $\partial\Omega(t)$, of which every point moves with the local fluid velocity \vec{V} . (See also Fig. 1.) If the volume $\Omega(t)$ is shrunk to a point, the resulting material volume is called a *fluid particle*. Consequently, the fluid properties of the fluid particle can be described mathematically in terms of space and time.

Under the assumption of the continuum mechanics, let χ be any continuous function, such as the density. The Reynolds transport theorem [11] gives the time rate of change of the "content" χ of Ω^* :

$$\frac{d}{dt} \int_{\Omega^*(t)} \chi dv = \int_{\Omega^*(t)} \frac{\partial \chi}{\partial t} dv + \int_{\partial\Omega^*(t)} \chi \vec{V}_b \cdot d\vec{S}, \quad (4)$$

where the element surface $d\vec{S}$ of Ω^* is moving with the velocity \vec{V}_b . Note that \vec{V}_b may vary over the surface $\partial\Omega^*$. Again, a special case is when the theorem is applied to the material volume $\Omega(t)$ with $\vec{V}_b = \vec{V}$.

The conservation laws (neglecting viscous fluxes for simplicity, without loss of generality in describing the approach) can be conveniently expressed over an arbitrary control volume $\Omega^*(t)$ in integral form:

$$\frac{d}{dt} \int_{\Omega^*(t)} \mathbf{U} dv + \int_{\partial\Omega^*(t)} [\mathbf{U}_c(\vec{V} - \vec{V}_b) + \vec{\mathbf{P}}_b] \cdot d\vec{S} = 0, \quad \text{with} \quad \vec{\mathbf{P}}_b = \vec{\mathbf{P}} + \begin{pmatrix} 0 \\ 0 \\ 0 \\ 0 \\ p\vec{V}_b \end{pmatrix}. \quad (5)$$

From the above equations, three fundamentally different approaches can result.

(5.1) *Eulerian Description:*

The Eulerian description assumes that the observer stays stationary with respect to the chosen frame of reference (e.g., inertial system). This requires:

$$\vec{V}_b = 0, \quad \text{and} \quad \Omega^* \neq \Omega^*(t). \quad (6)$$

That is, the control volume is fixed in time.

With the application of the Reynolds transport theorem Eq. (4), Eq. (5) is reverted to the familiar integral form:

$$\int_{\Omega^E} \frac{\partial \mathbf{U}}{\partial t} dv + \int_{\partial\Omega^E} [\mathbf{U}_c \vec{V} + \vec{\mathbf{P}}] \cdot d\vec{S} = 0, \quad (7)$$

where the superscript "E" is used to denote Eulerian frame of reference. In the discrete version of the above equation, each cell represents a control volume and is not moving in time, even though the flow may be unsteady. Note that the case in which an observer is fixed to a non-inertial frame, e.g. on rotating machines, also belongs to the Eulerian description.

(5.2) Lagrangian Description:

According to the strict definition, the Lagrangian description requires that the volume $\Omega^*(t)$ (enclosed by $\partial\Omega^*(t)$) move with the instantaneous fluid velocity and is identified as the material volume $\Omega(t)$ (see also Fig. 1). That is,

$$\vec{V}_b = \vec{V}, \quad \forall t > 0, \quad \text{and} \quad \Omega^*(t) = \Omega(t). \quad (8)$$

And the conservation laws are simplified to

$$\frac{d}{dt} \int_{\Omega(t)} \mathbf{U} dv + \int_{\partial\Omega(t)} \vec{\mathbf{P}}_b \bullet d\vec{\mathbf{S}} = 0. \quad (9)$$

Clearly, the pressure remains as the only contribution to the flux on the surface. This makes it extremely simple to calculate the time-rate of change of $\int \mathbf{U} dv$, i.e., involving only the pressure acting on the bounding surfaces. However, the trajectory of the vertices is the part that often causes difficulties, resulting in large deformation or irregularity. (See [1,2].) Nevertheless, this is a very intriguing idea that avoids the nonlinearity in the equation of motion, thus reducing many difficulties associated with the convective terms that exist only in the Eulerian viewpoint. Such nice properties unfortunately have not been able to outweigh the drawbacks (see Introduction) and gain favorable reception vs the Eulerian approach.

In the following, we propose a new approach that retains essential advantages of the above two approaches.

(5.3) Extended Lagrangian Description:

Close investigation of the surface integral reveals that the convective term can be eliminated also by requiring that:

$$(\vec{V} - \vec{V}_b) \bullet \vec{\mathbf{S}} = 0. \quad (10)$$

That is, a portion of the surface is parallel to $(\vec{V} - \vec{V}_b)$. Equation (5) then becomes,

$$\frac{d}{dt} \int_{\Omega^{EL}(t)} \mathbf{U} dv + \int_{\partial\Omega_{\vec{\mathbf{P}}}^{EL}(t)} \vec{\mathbf{P}}_b \bullet d\vec{\mathbf{S}} + \int_{\partial\Omega_{\vec{\mathbf{V}}}^{EL}(t)} [(\vec{V} - \vec{V}_b)\mathbf{U}_c + \vec{\mathbf{P}}_b] \bullet d\vec{\mathbf{S}} = 0. \quad (11)$$

The control volume now is denoted by superscript “EL” to indicate the present description. The surface $\partial\Omega^{EL}$ is comprised of two types, $\partial\Omega^{EL} = \partial\Omega_P^{EL} \cup \partial\Omega_V^{EL}$, where $\partial\Omega_P^{EL}$ coincides with the instantaneous particle paths and $\partial\Omega_V^{EL}$ represents the inflow and outflow faces. Clearly, the present “extended Lagrangian method” combines the quality of the above two approaches: the second surface integral includes both convective and pressure terms, as in the case of Eulerian approach; the first surface integral, on the other hand, merely has the effect of pressure, as in the case of Lagrangian approach. That is, see Fig. 2,

On $\partial\Omega_V^{EL} \leftarrow$ both convected and pressure fluxes

On $\partial\Omega_P^{EL} \leftarrow$ only pressure flux

For steady flow, $\vec{V}_b = 0$, there is no need for literally following particles because no variations of motion with time appear among the particles on the same streamline. Therefore that whether we strictly follow particles of same identity or not is irrelevant in the formulation. Indeed, following the streamlines, rather than particles, is the essence of the present approach and this rescues us from facing the difficulty of other Lagrangian approaches. Substituting $\vec{V}_b = 0$, in Eq. (11), we get

$$\frac{d}{dt} \int_{\Omega^{EL}} \mathbf{U} dv + \int_{\partial\Omega_P^{EL}} \vec{\mathbf{P}} \bullet d\vec{\mathbf{S}} + \int_{\partial\Omega_V^{EL}} [\mathbf{U}_c \vec{\mathbf{V}} + \vec{\mathbf{P}}] \bullet d\vec{\mathbf{S}} = 0, \quad \text{in } \Omega^{EL}. \quad (12a)$$

together with the constraint,

$$\vec{\mathbf{V}} \bullet \vec{\mathbf{S}} = 0, \quad \text{on } \partial\Omega_P^{EL}. \quad (12b)$$

For steady flow (fixed volume), the semi-discrete form, with the time-dependent term retained for iteration purpose, can be cast as:

$$\frac{d}{dt} \int_{\Omega^{EL}} \mathbf{U} dv + \sum_{i \in \partial\Omega_P^{EL}} \vec{\mathbf{P}}_i \bullet \vec{\mathbf{S}}_i + \sum_{i \in \partial\Omega_V^{EL}} \vec{\mathbf{F}}_i \bullet \vec{\mathbf{S}}_i = 0. \quad (13)$$

Examination of the above equations reveals some interesting insight. The imbalance of pressure in two neighboring cells with common interface boundary $\partial\Omega_P^{EL}$ causes the change of flow direction (i.e., $\partial\Omega_P^{EL}$) of the fluids under consideration as well as change of their volumes. In other words, the deformation and dilatation of the fluid can be described. Indeed, the Lagrangian grid includes multi-dimensional information and suggests how the fluid volume distorts in the flow. This point of view makes the description of fluid motion intuitively simple and clear. Moreover, it results in a major benefit in the numerical solution because this formulation avoids any arbitrary (numerical) mixing of fluids which in turn introduces numerical diffusion in the solution, notably across the contact discontinuity or shear layer. This diffusion error is common in the Eulerian formulation in which a nonstationary contact discontinuity is smeared without bound as time/space is marched. Furthermore, the advantage of the present approach is also clearly shown in its capability for crisply resolving multi-dimensional shocks.

To complete the numerical solution procedure in the finite volume, we employ an accurate and efficient new upwind scheme described in full detail in [12,13]. In what follows, we shall see that this new splitting has a very interesting bearing with the present extended Lagrangian method.

(5.4) *The Upwind Method*[12,13]

To illustrate the concept, it is sufficient to consider only the one-dimensional system. As a first step, by recognizing convection and pressure as two physically distinct (but coupled) processes, we split the flux in the form of Eq. (3). In other words, these two terms deserve separate treatments. Mathematically, we propose to separately deal with the genuinely nonlinear $((u - a, u + a)$ pair) and linearly degenerate (u) fields.

$$\mathbf{F} = u \begin{pmatrix} \rho \\ \rho u \\ \rho h_t \end{pmatrix} + \mathbf{P} = \mathbf{F}_c + \mathbf{P}, \quad \mathbf{F}_c = u \mathbf{U}_c. \quad (14)$$

The overhead arrow " $\overline{}$ " has been dropped for we are concerned only with one-dimensional flow. Both Mach number and velocity splittings can be used to represent the convective quantity u in \mathbf{F}_c . In most cases, there is virtually no difference between calculated results of the two splittings. As found in [13], the velocity splitting is more robust in calculating unsteady shock tube problems by allowing a larger time step at start. Now, the *numerical convective flux* at the interface (denoted by subscript $\frac{1}{2}$) straddling the left(L) and right(R) states, is effectively written as:

$$\mathbf{F}_{c1/2} = u_{1/2} \mathbf{U}_{cL/R}, \quad (15)$$

where $u_{1/2}$ is the interface convective velocity. Let $u_{1/2}$ be written as:

$$u_{1/2} = u_L^+ + u_R^-. \quad (16)$$

Several formulas are appropriate to define u^\pm , e.g.,

$$u^\pm = \begin{cases} (u \pm |u|)/2, & \text{if } |u| \geq a, \\ \pm(u \pm a)^2/4a, & \text{otherwise,} \end{cases} \quad (17)$$

where a is the speed of sound. The convectible variable vector \mathbf{U}_c is then upwinded solely based on the sign of $u_{1/2}$, viz,

$$\mathbf{U}_{cL/R} = \begin{cases} (\mathbf{U}_c)_L, & \text{if } u_{1/2} \geq 0, \\ (\mathbf{U}_c)_R, & \text{otherwise,} \end{cases} \quad (18)$$

We turn now to the pressure term by writing:

$$p_{1/2} = p_L^+ + p_R^-. \quad (19)$$

Similarly, a whole host of choices are possible for the pressure splitting. A differentiable pair of the '+' and '-' components have been found to be effective.

$$p^\pm = \begin{cases} p(1 \pm \text{sgn}(u))/2, & \text{if } |u| \geq a, \\ p(M \pm 1)^2(2 \mp M)/4, & \text{otherwise.} \end{cases} \quad (20)$$

This completes the definition of the numerical flux \mathbf{F} . Putting (15) and (19) together, we recast the interface flux in the following form:

$$\mathbf{F}_{1/2} = u_{1/2} \frac{1}{2}(\mathbf{U}_{cL} + \mathbf{U}_{cR}) - \frac{1}{2}|u_{1/2}| \Delta_{1/2}\mathbf{U}_c + \mathbf{P}_{1/2}. \quad (21)$$

where $\Delta_{1/2}\{\bullet\} = \{\bullet\}_R - \{\bullet\}_L$. Here the first term on the RHS is clearly *not* a simple average of the 'L' and 'R' fluxes, but rather a weighted average via the convective velocity. The dissipation term has merely a scalar coefficient $|u_{1/2}|$ and requires only $O(n)$ operations for an n -dimensional vector \mathbf{F} . Furthermore, since there is no differentiation (or jacobian matrix) involved in evaluating $\mathbf{F}_{1/2}$, the present method is easily extended to a general equation of state and non-equilibrium flows and the cost is only linearly increased with the additional conservation equations considered. Unlike the Roe or Osher schemes, the extension does not yield additional ambiguity such as the definition of averaged or intermediate states. Also, numerical tests strongly suggest an entropy-satisfying property by the present method.

To achieve higher-order spatial accuracy, a MUSCL-type procedure is followed to upwind-extrapolate variables(primitive variables in the calculations presented in this paper), with TVD limiters incorporated [14]. Then, a two-stage Runge-Kutta procedure is used to integrate the semi-discrete sytem Eq. (13), subject to the kinematic condition Eq. (12b).

The subsonic inflow conditions are imposed by specifying total enthalpy, total pressure, and flow angle, while the outflow conditions are obtained with specified static pressure and extrapolated total enthalpy, total pressure, and flow angle. The usual tangency procedure is used at the cell boundary that coincides with a physical wall—no ghost cells are used. The wall pressure is gotten using linear extrapolation from interior data, so is the total enthalpy.

6. MOTION OF LAGRANGIAN GRIDS

An important integral part of the present method is the grid motion that follows the constraint Eq. (12b). Two basic settings can be chosen for defining the motion of computational cells, namely the motion of cell centers or cell vertices. With the former approach the cell vertices will be defined by the position of neighboring centers, vice versa

for the latter. Since the constraint, Eq. (12b), is imposed on the cell boundary, it is consistent to determine the vertex motion instead. This is easily done with the velocity field known from the solution. The constraint Eq. (12b) is equivalent to the kinematic condition on a streamline:

$$\frac{dx}{u} = \frac{dy}{v} = \frac{dz}{w} \quad (22)$$

As flow variables are defined at cell centers, the velocity components at cell boundary must be defined by some interpolation procedure from surrounding cells. In the present report, we outline the general notion of grid movement and give a specific strategy showing how the grid is moved to meet the constraint for the test cases included in the paper. Let us consider the two-dimensional cell (i, j) , shown in Fig. 3. Three dimensional cells can be treated similarly. Assuming the cell boundary is described by a line segment $(\vec{r}_{i+1,j+1} - \vec{r}_{i,j+1})$. Since the segment is a part of a streamline, Eq. (22) gives

$$y_{i+1,j+1} = y_{i,j+1} + \bar{m}(x_{i+1,j+1} - x_{i,j+1}) \quad (23)$$

where

$$\bar{m} = \frac{\bar{v}}{\bar{u}}.$$

Here we list some possibilities for evaluating (\bar{u}, \bar{v}) :

(a) *Mid-point average*

$$\bar{\vec{V}} = \frac{1}{8}[2\vec{V}_{i,j} + 2\vec{V}_{i,j+1} + \vec{V}_{i+1,j} + \vec{V}_{i+1,j+1} + \vec{V}_{i-1,j} + \vec{V}_{i-1,j+1}], \quad (24a)$$

(b) *Upstream average*, assuming $u_{i,j} > 0, \forall i, j$,

$$\bar{\vec{V}} = \frac{1}{4}[\vec{V}_{i,j} + \vec{V}_{i,j+1} + \vec{V}_{i-1,j} + \vec{V}_{i-1,j+1}]. \quad (24b)$$

There are two unknowns, $(x, y)_{i+1,j+1}$, in Eq. (23). Another condition is needed to complete the system. In this report, we prescribe the value of x-coordinate for each i th grid line, i.e., $x = \text{constant}$ lines. This condition provides simplicity, but also yields accuracy as will be shown later. Furthermore, specification of x-coordinate allows one to put fine grids to resolve geometry details, e.g., near high curvature region.

When the constraint, Eq. (12b), is satisfied for all j th grid line, the conservation laws are basically solved in a one-dimensional stream tube, because there is no flow across the j -grid lines. As a result, high accuracy is expected with this virtually one-dimensional problem. This is the reason that the present method gives sharp representation for oblique shocks, as accurate as their counterpart in one-dimension. The formulation itself already inherits multi-dimensional information via the deformation of grid lines (i.e., streamlines).

The cost of arriving at the above constraint is negligible even if it is done at each iteration, because calculation of Eqs. (23) and (24) is all it needs. The grid motion can be predicted in phase as the evolution of the flow variables, or else for a prescribed number of flow variables iterations. However, it is unnecessary to adjust the grid so frequently while the flow is still evolving. A more thorough investigation about the optimal iteration per Lagrangian grid motion and its sensitivity to flow condition is useful, but is beyond the scope of the present paper.

7. TEST PROBLEMS AND DISCUSSION

We will show examples for flows at all speed regimes, featuring solution accuracy and grid aspects. The plots are organized uniformly for all cases presented. We show Mach contours overlaid on the grid used. Fine grids, by doubling grid number in both direction, are used only in the Eulerian calculation for comparison purpose. The grids shown are only one half of the whole grid in the Lagrangian case, and one quarter in the fine-grid case, thus corresponding to roughly the same location in both plots. The symbols denote the extended Lagrangian solutions and the lines are the Eulerian solutions. The Mach contours are chosen for presentation so that any numerical anomaly or inaccuracy can be more easily depicted than the other variables such as pressure.

The first example is the purely subsonic flow in which an $M_\infty = 0.4$ flow enters a channel with 20% circular bump, see Fig. 5 for detailed geometry. The Mach contours, given in Fig. 4, show nearly perfect symmetry about the midchord, except in the wake region. The wake region suggests an entropy production (numerical diffusion), likely due to numerical wall boundary condition, which to my knowledge is still a gray area in CFD. While this may be the situation, the Lagrangian solution still definitely results in a narrower wake, roughly half the width of the Eulerian result. The Eulerian solutions in fact have a slight asymmetry near the top wall, even though the residuals were dropped to machine zero. Notice that the computation domain is considered to be small, extending one chord length upstream and downstream from the bump, for this purely subsonic problem. It is worth noting that the present grid automatically evolves from initial Eulerian grid into the grid system seen in Fig. 4, according to Eqs. (23) and (24a). The grid spacing between streamlines increases near the stagnation points and converges as flow accelerates. The detailed distribution of variables on the top and bottom walls are plotted in Fig. 5. The fine-grid Eulerian solutions are included for comparison. The agreement is remarkable and again symmetry is quite evident. However, the fine-grid Eulerian solution over-predicts the stagnation pressure, whose theoretical value is 1.116, while the Lagrangian solution closely matches. Hereafter, for brevity and contrast to the Eulerian solution, we shall take the liberty of loosely using the term "Lagrangian solution" to mean the solution obtained by the extended Lagrangian method described in this paper—not in the strict Lagrangian sense. It is also noted that the fine-grid solution took considerably more iterations than the Lagrangian solution to converge.

The second example involves the popular test of transonic flow in a channel with 10% bump and $M_\infty = 0.675$. Results are given in Figs. 6 and 7. Again, we show the Mach contours and distributions on both walls. The agreement of the coarse-grid Lagrangian solutions with the fine-grid Eulerian solutions is excellent. The shock resolution from the Lagrangian method is outstanding, so is the prediction of the so-called "Zierep" singularity at the foot of the shock on the curved surface. The Lagrangian solution again yields a grid that senses the global flow characteristic. Notice that no clustering of grid is necessary to capture the shock in the correct location.

The next case is also a standard one, involving an $M_\infty = 1.4$ flow and 4% bump. This case consists of small subsonic pocket resulting from short Mach stems on both walls, shown in Fig. 8. Shock-shock-expansion waves interactions take place behind the trailing edge. The shock locations are in excellent agreement with the fine-grid solutions. Close examination of the Lagrangian grid shows that the grid lines (also streamlines) remain straight until the shock is encountered, as it should. The Eulerian grid however already began bending at the leading edge for all j -th lines, simply because of geometry constraint. The present method yields grids that are conforming with the flow features by bending, expanding/contracting. The net result is that excellent shock resolution is obtained, even though the shock is oblique to the grid line. Figure 9 displays a one-cell capturing of the oblique shock. This is not entirely surprising since the present formulation has already taken account of the multi-dimensional nature of the flow via the streamline deformation caused by the fluxes (pressure forces) of surrounding fluids.

The fourth test is an $M_\infty = 1.8$ flow over a 15° ramp. This case consists of a Mach stem about 10% of channel height, a slip line emanating from the triple point, and reflected shocks. In Fig. 10, the mach contours depict an overall picture of the flow, demonstrating a sharp resolution of the ramp shock, Mach stem, and the subsequent shocks. The slip line, whose strength is being weakened by the expansion wave generated at the ramp shoulder and transmitted through the first reflected shock, is resolved to the same level of accuracy as given by the fine-grid solution, i.e., with the same level of spatial spreading. Figure 11 vividly displays how the grid lines bend as the shock is encountered and change direction according to the flow. The grid itself already suggests the flow structures, train of shock reflections, expansions, as well as the Mach stem across which there is no change of flow angle. It is worth noting the clear slipline emanating from the triple point. In contrast to the shock-aligned grid, the present grid is aligned with the streamlines, which will never cross each other, but the shocks can. Thus the present method is indifferent to whether the high-gradient regions intersect. The profiles (Fig. 12) on the walls show good agreement of both solutions. Excellent shock resolution capability is observed on both walls even the second reflected shocks remain well resolved.

CONCLUDING REMARKS

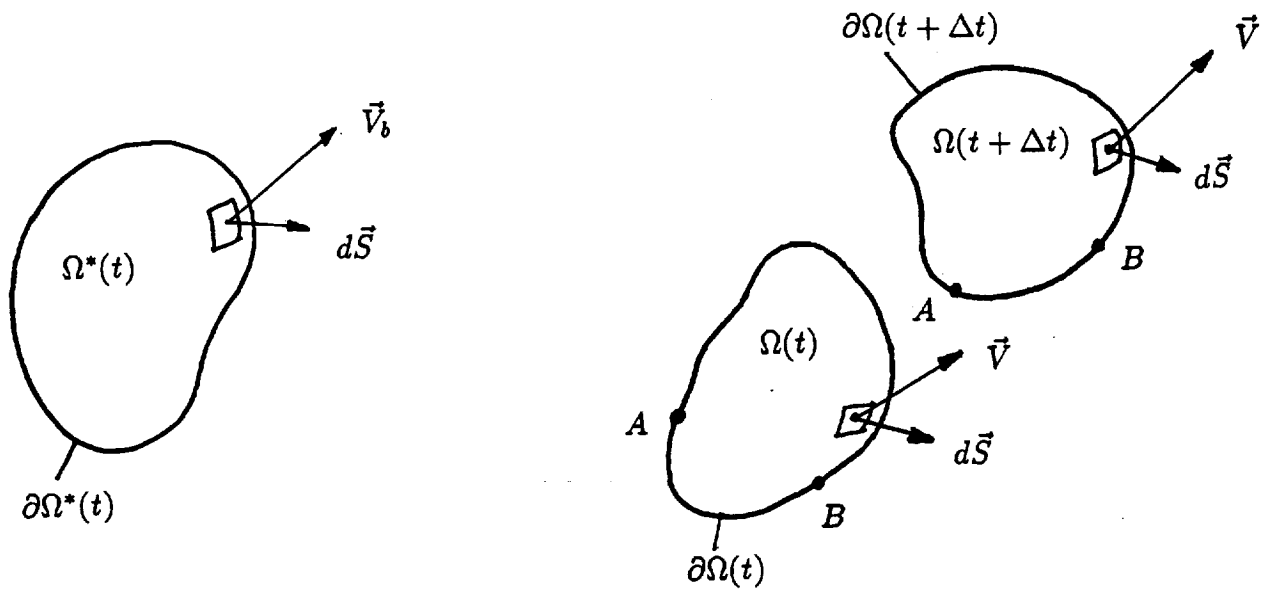
We have presented a unique formulation for dealing with *subsonic* as well as supersonic flows. The method, referred to as extended Lagrangian method, combines the accuracy

belonging to a Lagrangian description and the robustness and simplicity of an Eulerian description. Through systematic comparison with fine-grid solutions and a theoretical check for flows at various regimes, we have demonstrated its capability for crisply capturing high-gradient regions that are not aligned with the grid. In contrast to adaptive approaches reported to date, the present approach already automatically inherits the ability to adapt to flow features, but based on an entirely different adaptive philosophy in which there is no need for clustering grid lines. Since the grid lines are not aligned with high-gradient areas, they are maintained regular and uniform. Moreover, one set of grid lines that coincides with streamlines depicts vividly a form of "numerical flow visualization". Without resorting to arbitrary detecting criteria, the present approach not only predicts well the nonlinear waves, such as shock and rarefaction waves, but also is especially amenable to treating a linearly degenerate field, such as a contact discontinuity. Furthermore, since the grid spacing is maintained relatively uniform, a large time step is permitted throughout the calculation, thus increasing efficiency. Also the common adaptive strategy will have great difficulty in the case of intersecting shocks, because the grid lines will cross each other, if not checked. We also suggest that the present extended Lagrangian method is a viable alternative approach to the current multi-dimensional scheme and grid-enriching adaptive procedure for complex flows having high-gradient regions. In fact it is an elegant and effortless approach to deal with multi-dimensional flows. Further development and 3D applications are currently underway and will be reported in the future.

REFERENCES

1. Hirt, C. W., Amsden, A. A., and Cook, J. L., "An Arbitrary Lagrangian-Eulerian Computing Method for all Flow Speeds," *J. Comput. Phys.* **14**, 227 (1974).
2. Pracht, W., "Calculating Three-Dimensional Fluid Flows at All Speeds with an Eulerian-Lagrangian Computing Mesh," *J. Comput. Phys.* **17**, 132 (1975).
3. Loh, C. Y. and Hui, W. H., "A New Lagrangian Method for Steady Supersonic Flow Computation I. Gudonov Scheme," *J. Comput. Phys.* **89**, 207 (1990).
4. Loh, C. Y. and Liou, M.-S., "A New Lagrangian Method for Three-dimensional Steady Supersonic Flow," submitted for publication.
5. Gudonov, S. K., "A Difference Method for the Numerical Calculation of Discontinuous Solutions of Hydrodynamic Equations," *Mat. Sb.* **47**, 271 (1959).
6. Loh, C. Y. and Liou, M.-S., "Lagrangian Solution of Supersonic Real Gas Flow," *J. Comput. Phys.* **104**, 150 (1993).
7. Harten A., "ENO Schemes with Subcell Resolution," *J. Comput. Phys.* **83**, 148 (1989).
8. Addressio, F. L. et al, "CAVEAT:A Computer Code for Fluid Dynamics Problems with Large Distortion and Internal Slip," Los Alamos National Laboratory, LA-10613-MS, 1986.

9. Amsden, A. A., Rourke, P. J., and Butler, T. D., "KIVA-II:A Computer Program for Chemically Reactive Flows with Sprays," Los Alamos National Laboratory, LA-11560-MS, 1989.
10. Hui, W. H. and Van Roessel, H., "Unsteady Three-Dimensional Flow Theory via Material Functions," in *AGARD Symposium on Unsteady Aerodynamics-Fundamentals and Application to Aircraft Dynamics, Götting, West Germany, 1985*, S1, CP-386.
11. Thompson, P. A., *Compressible-Fluid Dynamics*, p.15, McGraw-Hill, 1972.
12. Liou, M.-S. and Steffen, C. J., "A New Flux Splitting Scheme," NASA TM 104404, 1991; also to appear in *J. Comput. Phys.*
13. Liou, M.-S., "On a New Class of Flux Splittings," *Lecture Notes in Physics 414*, pp.115-119, Springer-Verlag, 1993.
14. Liou, M.-S., and Hsu, A. T. "A Time Accurate Finite Volume High Resolution Scheme for Three Dimensional Navier-Stokes Equations," AIAA paper 89-1994-CP, 1989.



Control volume, denoted by “*”, may be nonstationary, e.g., on rotating frame.

Material volume, $\vec{V}_b = \vec{V}$

Fig. 1. Definition of a control volume and material volume.

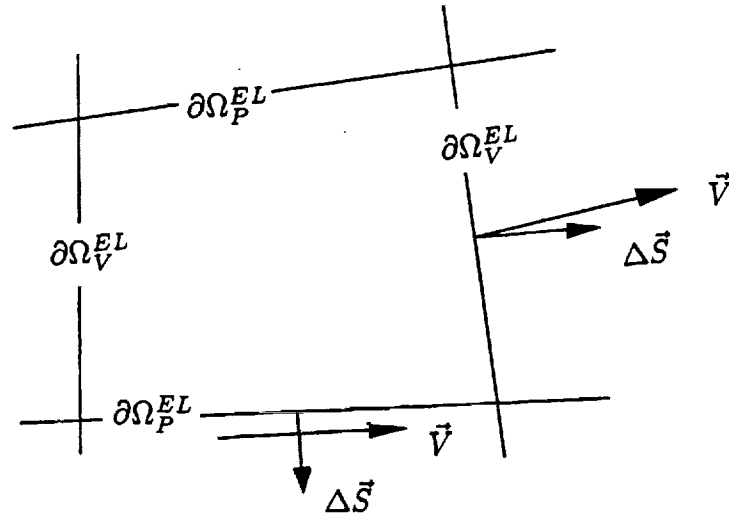


Fig. 2. Definition of an Extended Lagrangian volume: the cell boundary $\partial\Omega_P^{EL}$ is parallel to the fluid velocity.

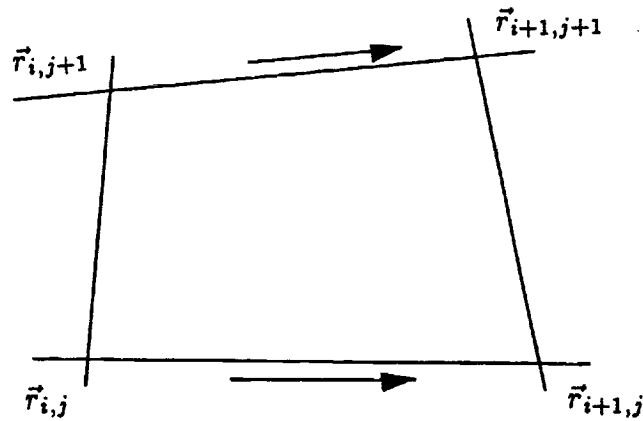


Fig. 3. Generating a Lagrangian computational cell so that the cell boundary $(\vec{r}_{i+1,j+1} - \vec{r}_{i,j+1})$ is parallel to \vec{V} .

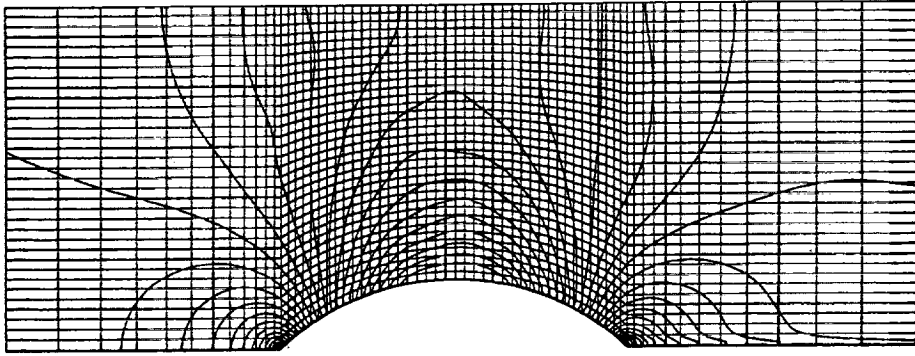
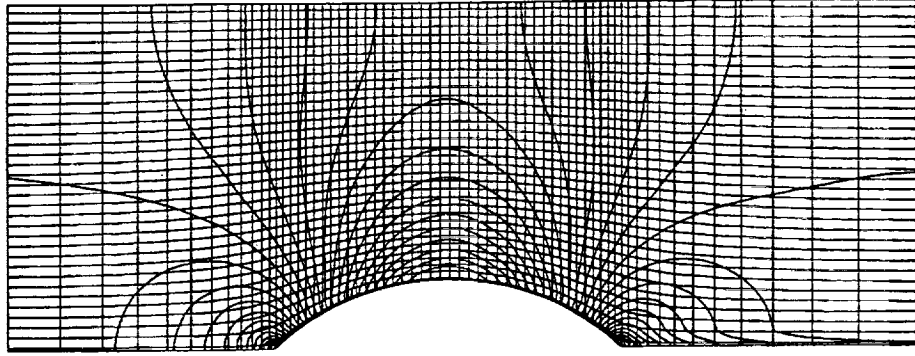


Fig. 4. Mach contours for $M_\infty = 0.4$, 20% bump flow; (a) Lagrangian solution (134×70 grid), (b) Eulerian solution (266×138 grid). (Contour levels: $M_{min} = 0.0$, $M_{max} = 0.8$, $\Delta M = 0.02$.)

20% BUMP ON A CHANNEL

$M_\infty = 0.4$

$O(h^2)$, 134×70 & 266×138 (—)

Δ Top wall, \circ Bottom wall

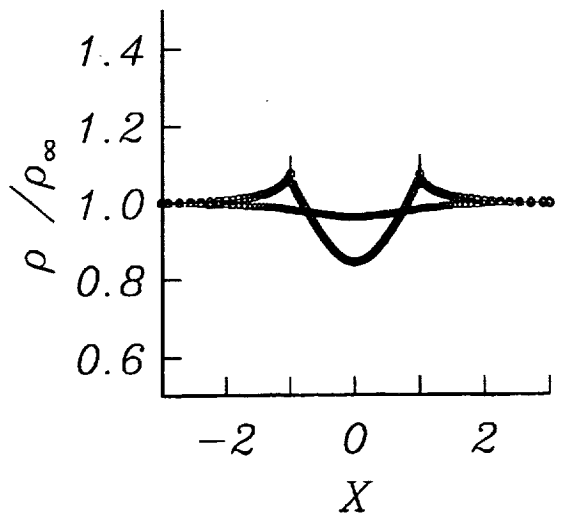
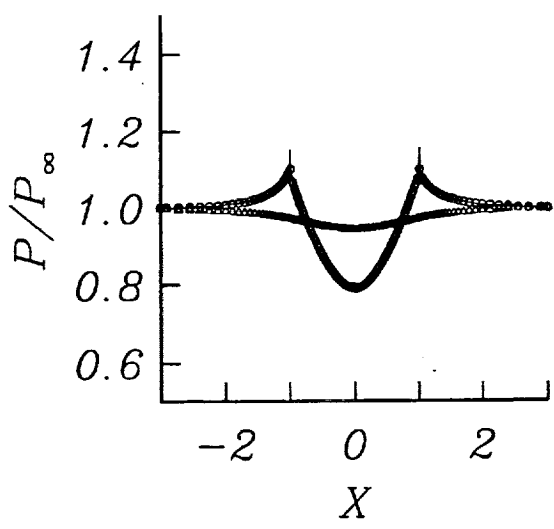
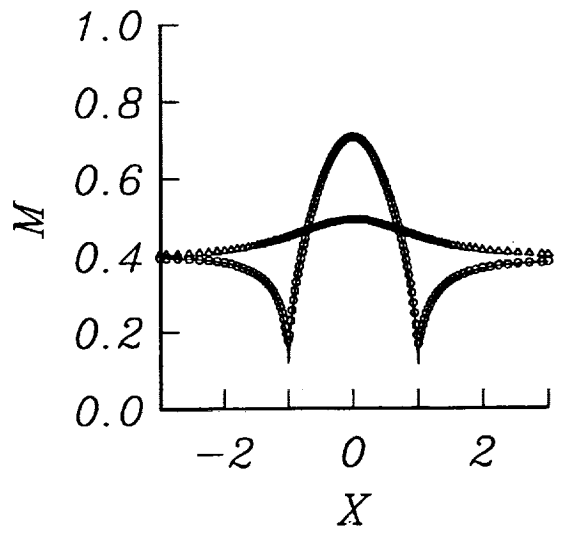
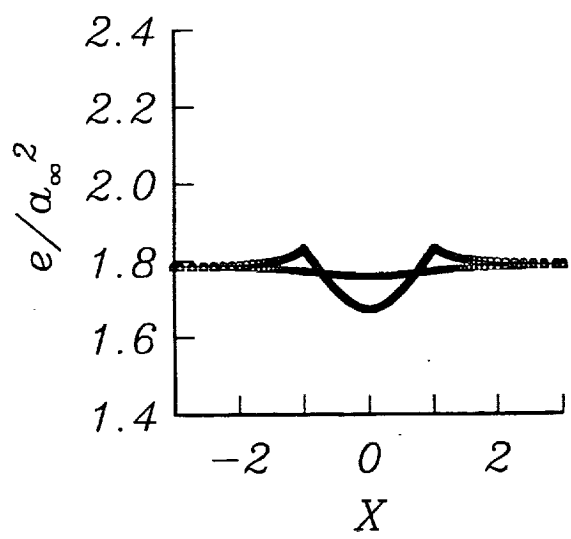
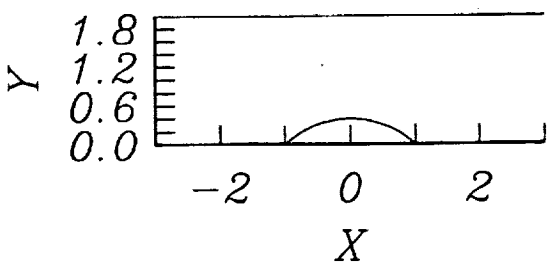


Fig. 5. Distributions of variables on top and bottom walls for $M_\infty = 0.4$, 20% bump flow; lines are Eulerian solution (266×138 grid) and symbols are Lagrangian solution (134×70 grid) with Δ and \circ denoting top and bottom walls respectively.

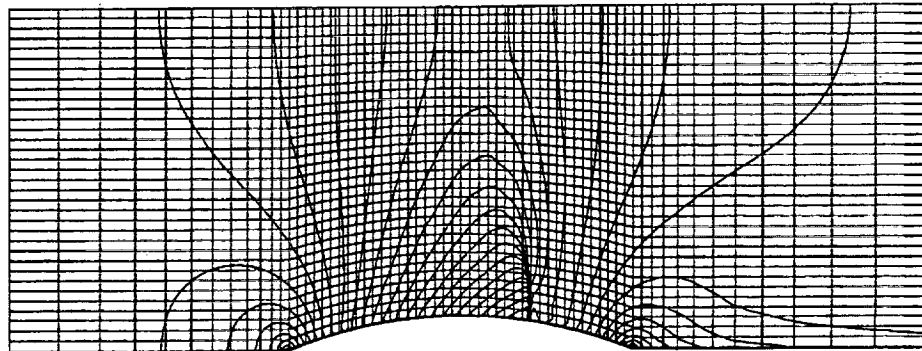
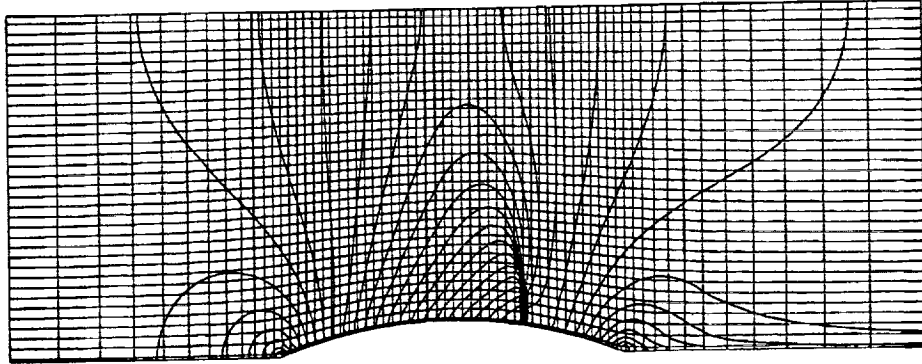
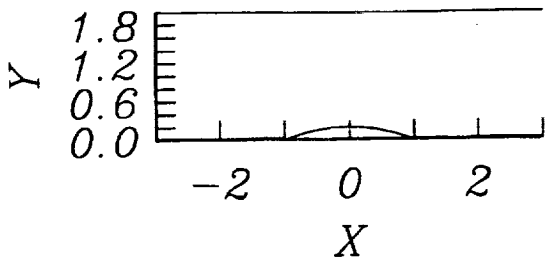


Fig. 6. Mach contours for $M_\infty = 0.675$, 10% bump flow; (a) Lagrangian solution (134×70 grid), (b) Eulerian solution (266×138 grid). (Contour levels: $M_{min} = 0.0$, $M_{max} = 1.6$, $\Delta M = 0.04$.)



10% BUMP ON A CHANNEL

$$M_\infty = 0.675$$

$O(h^2)$, 134×70 & 266×138 (—)

Δ Top wall, \circ Bottom wall

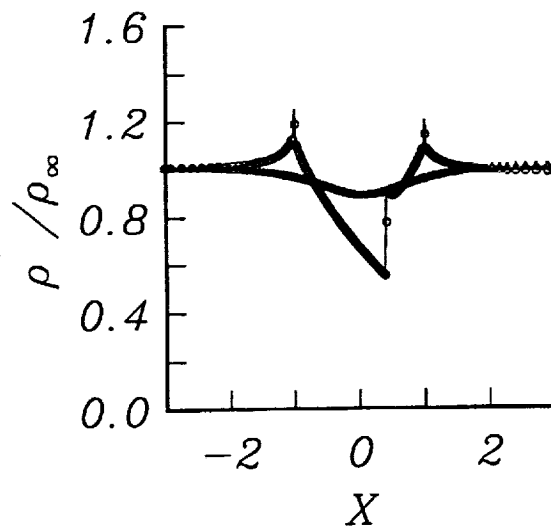
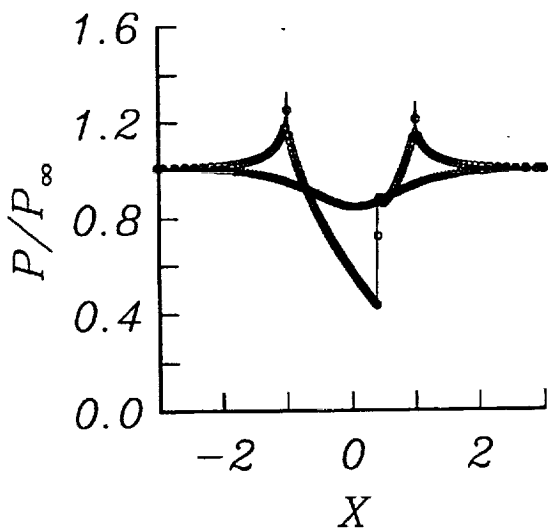
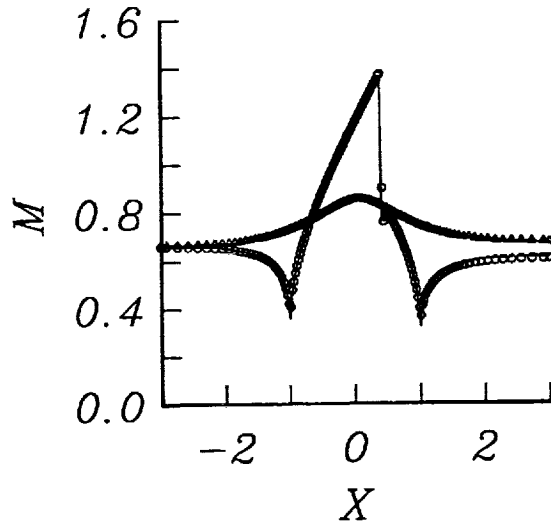
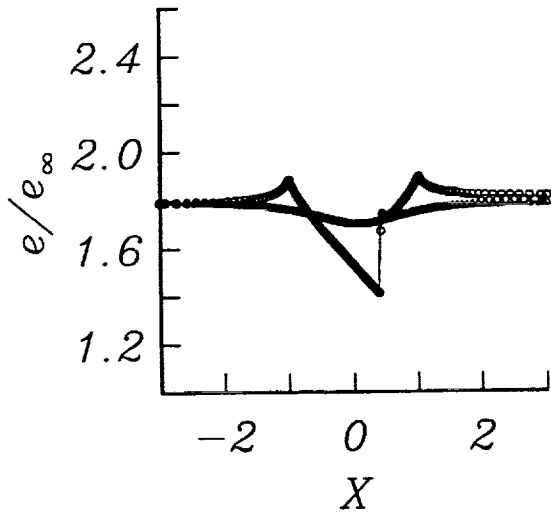


Fig. 7. Distributions of variables on top and bottom walls for $M_\infty = 0.675$, 10% bump flow; lines are Eulerian solution (266×138 grid) and symbols are Lagrangian solution (134×70 grid) with Δ and \circ denoting top and bottom walls respectively.

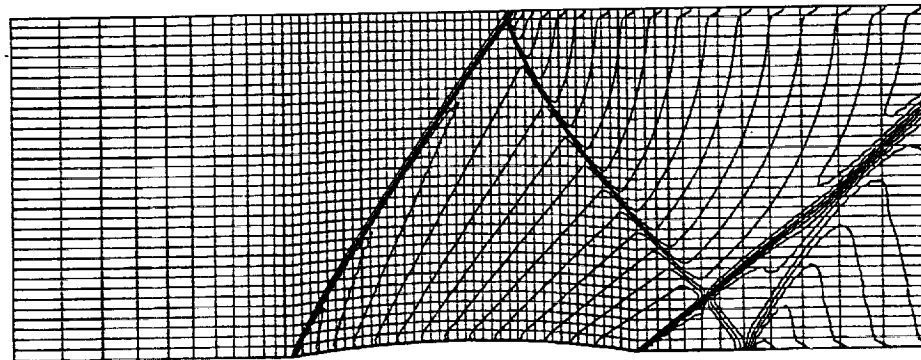
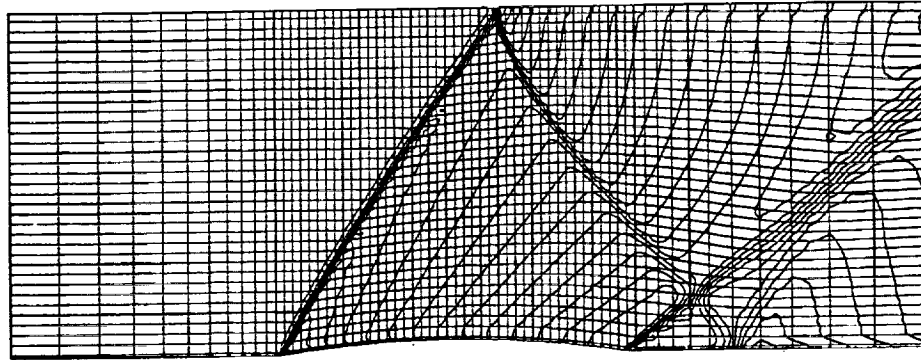
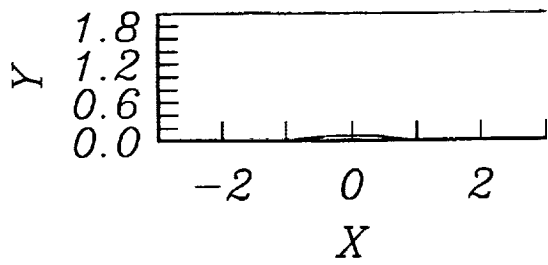


Fig. 8. Mach contours for $M_\infty = 1.4$, 4% bump flow; (a) Lagrangian solution (134×70 grid), (b) Eulerian solution (266×138 grid). (Contour levels: $M_{min} = 0.4$, $M_{max} = 2.2$, $\Delta M = 0.045$.)



4% BUMP ON A CHANNEL

$M_\infty = 1.4$

$O(h^2)$, 134×70 & 266×138 (—)

Δ Top wall, \circ Bottom wall

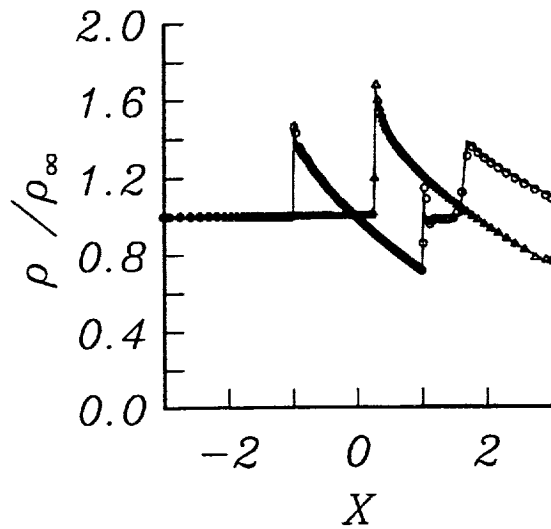
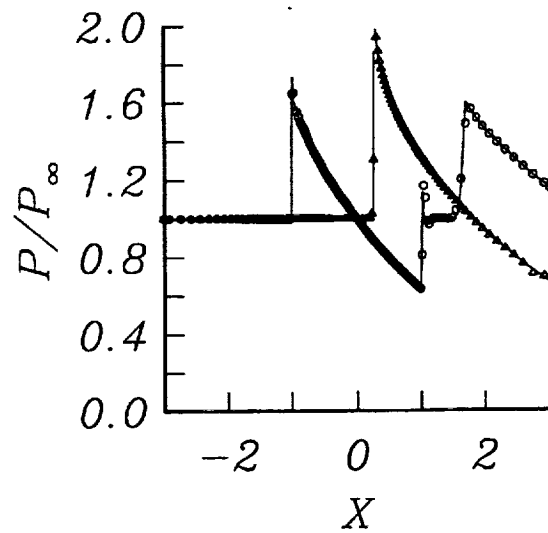
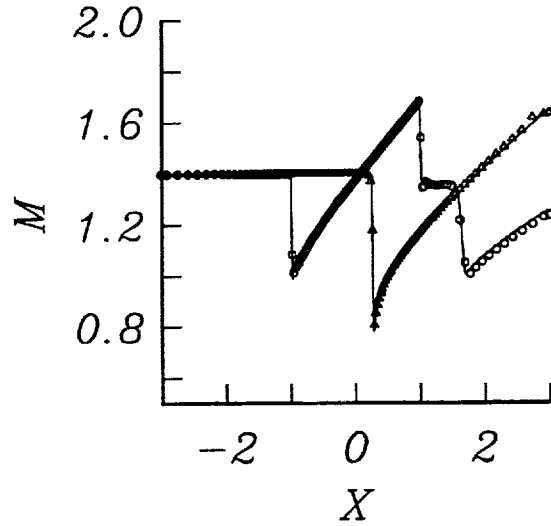
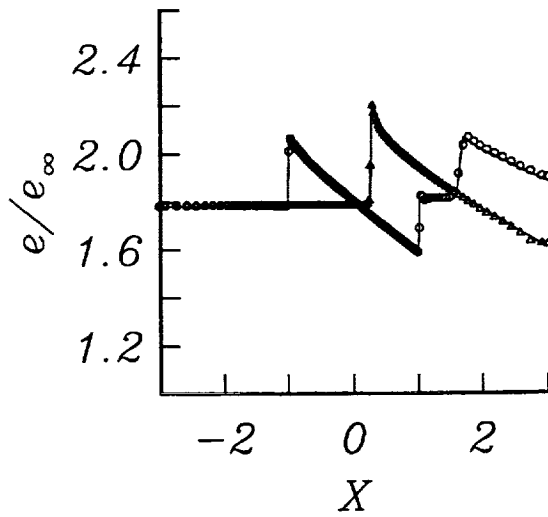


Fig. 9. Distributions of variables on top and bottom walls for $M_\infty = 1.4$, 4% bump flow; lines are Eulerian solution (266×138 grid) and symbols are Lagrangian solution (134×70 grid) with Δ and \circ denoting top and bottom walls respectively.

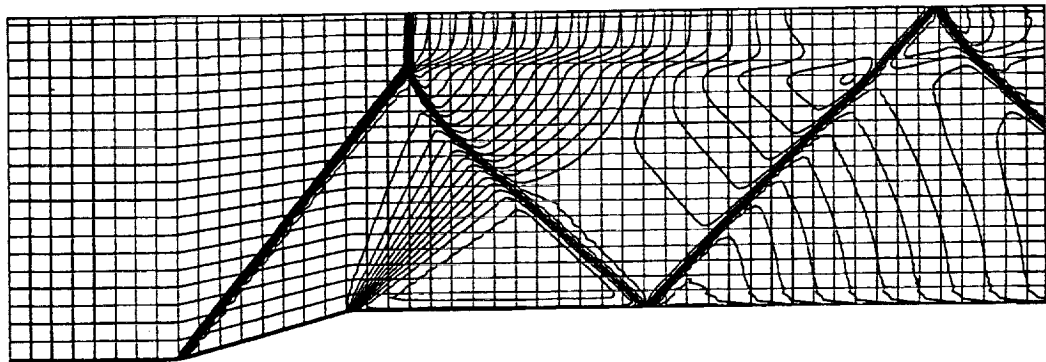
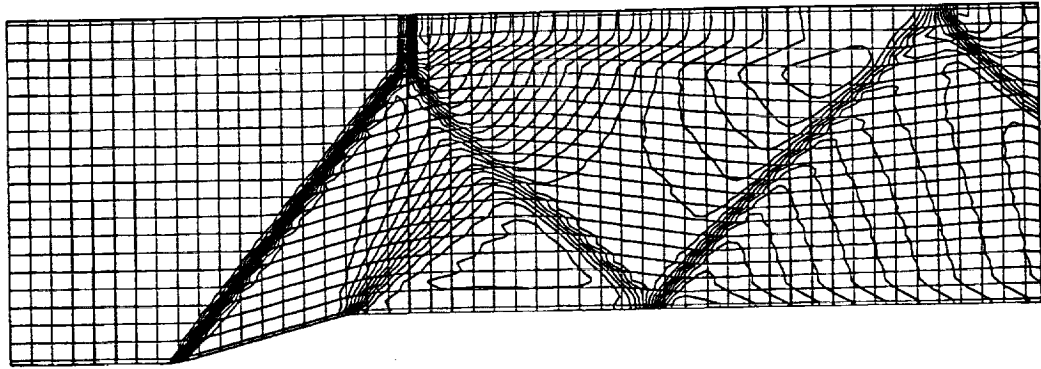


Fig. 10. Mach contours for $M_\infty = 1.8$, 15° ramp flow; (a) Lagrangian solution (100×41 grid), (b) Eulerian solution (198×80 grid). (Contour levels: $M_{min} = 0.4$, $M_{max} = 2.2$, $\Delta M = 0.045$.)

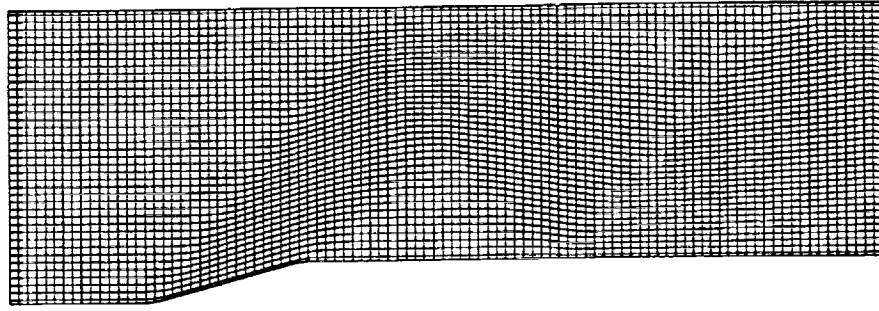


Fig. 11. Lagrangian grid, showing streamlines and the trains of shock and expansion waves.

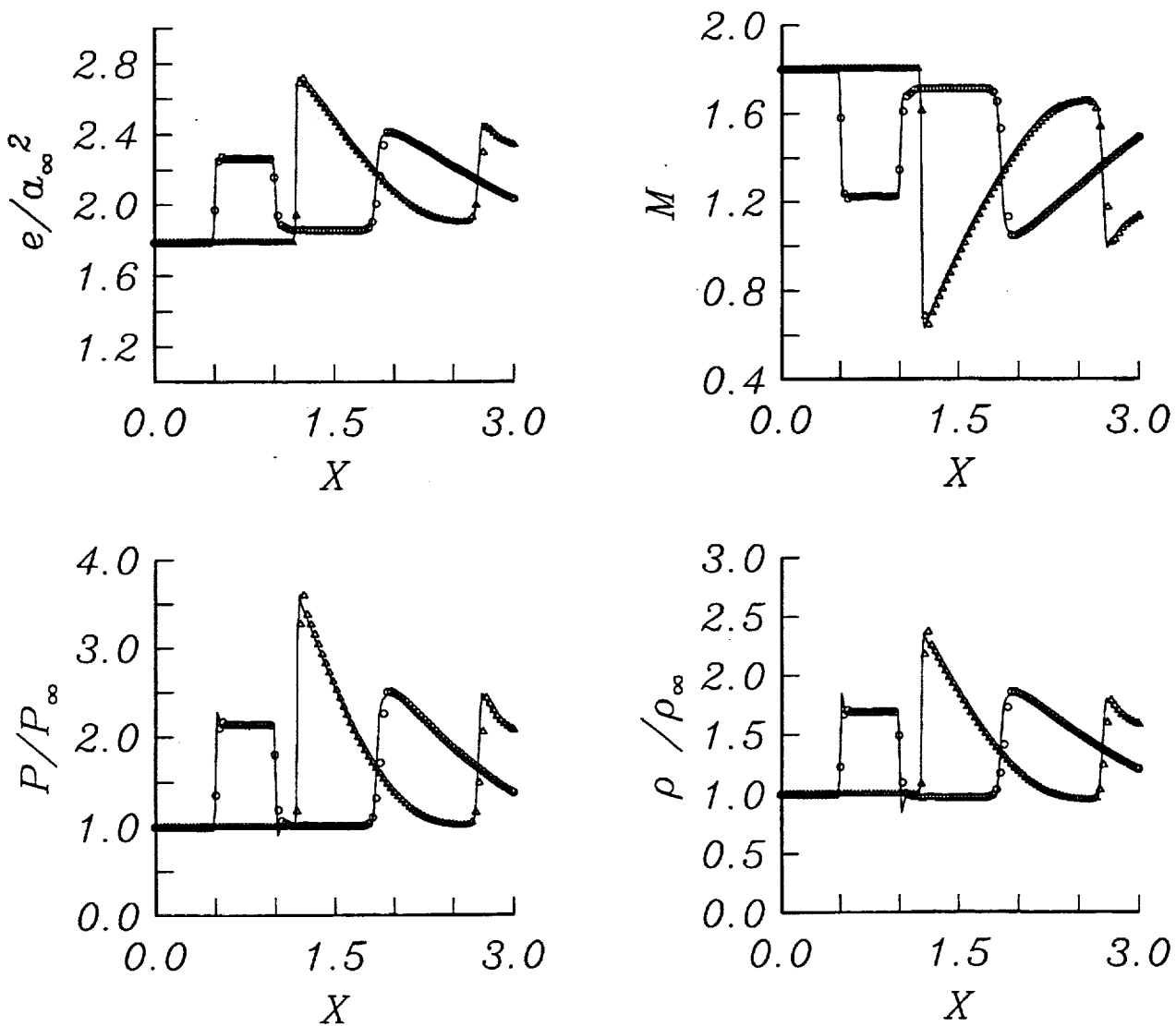


Fig. 12. Distributions of variables on top and bottom walls for $M_\infty = 1.8$, 15° ramp flow; lines are Eulerian solution (198×80 grid) and symbols are Lagrangian solution (100×41 grid) with Δ and \circ denoting top and bottom walls respectively.

REPORT DOCUMENTATION PAGE

Form Approved
OMB No. 0704-0188

Public reporting burden for this collection of information is estimated to average 1 hour per response, including the time for reviewing instructions, searching existing data sources, gathering and maintaining the data needed, and completing and reviewing the collection of information. Send comments regarding this burden estimate or any other aspect of this collection of information, including suggestions for reducing this burden, to Washington Headquarters Services, Directorate for Information Operations and Reports, 1215 Jefferson Davis Highway, Suite 1204, Arlington, VA 22202-4302, and to the Office of Management and Budget, Paperwork Reduction Project (0704-0188), Washington, DC 20503.

1. AGENCY USE ONLY (Leave blank)	2. REPORT DATE May 1992	3. REPORT TYPE AND DATES COVERED Technical Memorandum	
4. TITLE AND SUBTITLE An Extended Lagrangian Method		5. FUNDING NUMBERS WU-505-62-52	
6. AUTHOR(S) Meng-Sing Liou		8. PERFORMING ORGANIZATION REPORT NUMBER E-7798	
7. PERFORMING ORGANIZATION NAME(S) AND ADDRESS(ES) National Aeronautics and Space Administration Lewis Research Center Cleveland, Ohio 44135-3191		10. SPONSORING/MONITORING AGENCY REPORT NUMBER NASA TM-106129	
9. SPONSORING/MONITORING AGENCY NAME(S) AND ADDRESS(ES) National Aeronautics and Space Administration Washington, D.C. 20546-0001		11. SUPPLEMENTARY NOTES Responsible person, Meng-Sing Liou, (216) 433-5855.	
12a. DISTRIBUTION/AVAILABILITY STATEMENT Unclassified - Unlimited Subject Category 34		12b. DISTRIBUTION CODE	
13. ABSTRACT (Maximum 200 words) A unique formulation of describing fluid motion is presented. The method, referred to as "extended Lagrangian method," is interesting from both theoretical and numerical points of view. The formulation offers accuracy in numerical solution by avoiding numerical diffusion resulting from mixing of fluxes in the Eulerian description. Meanwhile, it also avoids the inaccuracy incurred due to geometry and variable interpolations used by the previous Lagrangian methods [1,2]. Unlike the Lagrangian method proposed in [3,4] which is valid only for supersonic flows, the present method is general and capable of treating subsonic flows as well as supersonic flows. The method proposed in this paper is robust and stable. It automatically adapts to flow features without resorting to clustering, thereby maintaining rather uniform grid spacing throughout and large time step. Moreover, the method is shown to resolve multi-dimensional discontinuities with a high level of accuracy, similar to that found in one-dimensional problems.			
14. SUBJECT TERMS Lagrangian description; Solution adaptation; Flux splitting		15. NUMBER OF PAGES 28	
17. SECURITY CLASSIFICATION OF REPORT Unclassified		16. PRICE CODE A03	
18. SECURITY CLASSIFICATION OF THIS PAGE Unclassified	19. SECURITY CLASSIFICATION OF ABSTRACT Unclassified	20. LIMITATION OF ABSTRACT	

